

Synthesis, structures, and photoluminescent properties of two ligand unsupported silver(I) coordination polymers from isonicotinate anions

Zheng Liu,^{ab} Ping Liu,^{*a} Yun Chen,^{ab} Jian Wang^a and Meihua Huang^{ab}

^a Fujian Institute of Research on the Structure of Matter, Chinese Academy of Sciences, Fuzhou, Fujian, 350002, P. R. China. E-mail: pliu@fjirsm.ac.cn; Fax: 86-591-83714648; Tel: 86-591-83704960

^b Graduate School of Chinese Academy of Sciences, Beijing, 100039, P. R. China

Received (in Durham UK) 15th November 2004, Accepted 5th January 2005
First published as an Advance Article on the web 18th January 2005

Assembly of isonicotinate acid (HL) and Ag(I) by a layer-separating diffusion method at ambient temperature gave rise to two novel structural coordination polymers with ligand unsupported Ag⁺⋯Ag interactions, namely, [(Ag₄L₄)·H₂O·0.5CH₃OH]_n (**1**) and [(Ag₃L₂)NO₃]_n (**2**). Compound **1** is the first example of double-layer architecture and features an alternative stacking mode with Ag⁺⋯Ag interactions, π–π interactions and Ag⁺⋯O interactions. The synthesis of compound **2** offered us an opportunity to study the role of counteranions in Ag⁺⋯Ag interactions. Both compounds display intense room temperature photoluminescence in the solid state.

Introduction

One of the thematic issues in silver(I) chemistry is the understanding of close-shell d¹⁰ Ag⁺⋯Ag interactions that give rise to intriguing supramolecular motifs, crystal packing, and specific photophysical properties.¹ Recent research has shown that direct metal–metal interactions are one of the most important factors for the manifestation of such properties.^{2,3} Particularly due to the limitation of evidence involving the existence of weak Ag(I)⋯Ag(I) attractive interactions in the absence of any supportive bridging ligation,⁴ the induction and modulation of such metal–metal interactions has become a more challenging field. As is already known, isonicotinate anions possess the capability to chelate and bridge metal atoms in various coordination modes using the carboxylate oxygen atoms and nitrogen atom of the pyridyl ring.⁵ Unfortunately, silver(I) complexes with such heterocyclic aromatic carboxylate ligands exhibiting short Ag⁺⋯Ag separations were scarce, and only a few examples have been reported.^{6,16} On the other hand, it is widely acknowledged that self-assembly of coordination frameworks is highly influenced by factors such as the solvent system, template, pH value of the solution, and steric requirement of the counterion.⁷ Herein, we synthesized two new silver(I) coordination polymers [(Ag₄L₄)·H₂O·0.5CH₃OH]_n (**1**), and [(Ag₃L₂)NO₃]_n (**2**) (HL = isonicotinate acid) by controlling the pH value of the solution. To the best of our knowledge, **1** was the first example of double-layer architecture until now and displays intense photoluminescence in the solid state at room temperature.

Experimental

General

All reagents were analytical grade and used as received. The IR spectra were recorded as KBr discs on a Magna 750 FT-IR spectrometer. C, H and N microanalyses were performed on a Vario EL III elemental analyzer. Thermogravimetric analyses were performed on a Perkin Elmer TGA/SDTA851 instru-

ment. Fluorescent analyses were performed on an Edinburgh Instruments analyzer model FL920. XRPD data were collected on an Xpert MPD diffractometer at room temperature.

Synthesis

[(Ag₄L₄)·H₂O·0.5CH₃OH]_n (**1**). A solution of L[−] (0.012 g, 0.10 mmol) in MeOH (5 ml), which achieved the pH value of 9 by neutralizing KOH with HL, was carefully layered on a solution of AgNO₃ (0.017 g, 0.10 mmol) in H₂O (5 ml). Diffusion between the two phases over a period of two weeks produced colorless block crystals. For **1**, yield: 56%. Calc. for C_{24.5}H₂₀Ag₄N₄O_{9.5}: C 30.85, H 2.11, N 5.87%; found: C 31.32, H 1.76, N 6.07%.

[(Ag₃L₂)NO₃]_n (**2**). A solution of L[−] (0.012 g, 0.10 mmol) in MeOH (5 ml), which achieved the pH value of 7 by neutralizing KOH with HL, was carefully layered on a solution of AgNO₃ (0.017 g, 0.10 mmol) in H₂O (5 ml). Diffusion between the two phases over a period of two weeks produced colorless block crystals. For **2**, yield: 71%. Calc. for C₁₂H₈Ag₃N₃O₇: C 22.88, H 1.28, N 6.67%; found: C 22.27, H 1.27, N 6.66%.

X-Ray crystallography

Single crystals of complexes **1** and **2** with approximate dimensions 0.18 × 0.15 × 0.12 mm (**1**) and 0.40 × 0.20 × 0.20 mm (**2**) were used for X-ray diffraction analyses. Data were collected on a Bruker Smart Apex CCD diffractometer with Mo–Kα radiation (λ = 0.71073 Å) at 173(2) K. Empirical absorption corrections were applied by using the SADABS program for the Siemens area detector. The structures were solved with direct methods and all calculations were performed using the SHELXTL package.⁸ The structures were refined by full-matrix least squares with anisotropic thermal parameters for non-hydrogen atoms. For **1**, water H-atom coordinates were located from difference maps and refined isotropically, the O–H distances involving the water molecules were refined

Table 1 Crystal data and refinement parameters of **1** and **2**

	1	2
Formula	C _{24.5} H ₂₀ Ag ₄ N ₄ O _{9.5}	C ₁₂ H ₈ Ag ₃ N ₃ O ₇
FW	953.93	629.82
Crystal system	Triclinic	Triclinic
Space group	<i>P</i> 1	<i>P</i> 1
<i>T</i> /K	173(2)	173(2)
<i>a</i> /Å	8.6509(12)	8.1686(16)
<i>b</i> /Å	12.618(2)	10.4479(18)
<i>c</i> /Å	14.000(3)	10.8106(17)
α /°	107.936(10)	62.257(7)
β /°	99.633(6)	69.159(7)
γ /°	90.210(7)	80.817(9)
<i>U</i> /Å ³	1430.9(4)	763.1(2)
<i>Z</i>	2	2
μ /mm ⁻¹	2.757	3.855
Reflections collected	10946	5762
Reflections unique	6442	3399
<i>R</i> _{int}	0.0160	0.0169
<i>R</i> ₁ ^a [<i>I</i> > 2σ(<i>I</i>)]	0.0373	0.0224
<i>wR</i> ₂ ^a [<i>I</i> > 2σ(<i>I</i>)]	0.0829	0.0568
Max., min. ρ/e Å ⁻³	1.522, -1.028	0.869, -1.207

$$^a R_1 = \Sigma ||F_o| - |F_c|| / \Sigma |F_o|; wR_2 = [\Sigma w(F_o^2 - F_c^2)^2 / \Sigma w(F_o^4)]^{1/2}.$$

with a DFIX restraint of 0.85 Å. Other hydrogen atoms were generated geometrically and treated as riding. For **2**, all hydrogen atoms were generated geometrically and treated as riding. The crystallographic data for **1** and **2** are summarized in Table 1, and the selected bond distances and angles are listed in Table 2.†

Results and discussion

Synthesis

The colorless crystals **1** and **2** were both synthesized by the reaction of AgNO₃ in H₂O with L⁻ in CH₃OH *via* a liquid diffusion method. The main synthetic difference between **1** and **2** consisted in the value of pH, 9 for **1**, and 7 for **2**, respectively. As demonstrated previously, it is possible to control the deprotonation of different labile hydrogen atoms attached to the oxygen or nitrogen atoms at different pH levels and hence tune the coordination mode.⁹ It should be mentioned that previously reported isonicotinate acid with Ag(I) frequently employed no μ₃-bridge mode,¹⁰ which may be ascribed to the fact that related compounds were produced under a lower reaction pH value. This fact encouraged us to adjust the solution acidity to obtain new silver(I) cluster-based coordination polymers. As expected, L⁻ in both **1** and **2** adopted a μ₃-bridge mode under high pH value conditions. However, the pH difference between **1** and **2** led to the fact that, according to the number of Ag(I) in the two reaction systems, there are more μ₃-bridge L⁻s in **1** than in **2**, which resulted in the phenomenon in which every Ag(I) in **1** coordinated with two oxygen atoms from two different ligands and one nitrogen atom from the third ligand, instead of only two ligands coordinating with Ag(I) in **2** by two oxygen atoms or one oxygen atom and one nitrogen atom. This work demonstrates that, besides increasing the coordination sites of the ligands, the change of pH value in high scope (pH ≥ 7) could lead to a larger number of this kind of ligands. In addition, the purity of complexes **1** and **2** was confirmed by X-ray powder diffraction analyses, in which the lattice parameters derived from XRPD data are almost consistent with those obtained by single crystal X-ray diffraction.

† CCDC reference numbers 253118 for **1** and 253117 for **2**. See <http://www.rsc.org/suppdata/nj/b4/b417363e/> for crystallographic data in .cif or other electronic format.

Crystal structures

The structure of **1** has been established by crystallography. As shown in Fig. 1, each Ag(I) ion features a T-shaped geometry, being coordinated by two oxygen atoms from different L⁻ ligands and a nitrogen atom from the third L⁻ (neglecting the Ag...Ag interaction). The bond distances of Ag–O [ranging from 2.233(3) Å for Ag(1)–O(7) to 2.283(4) Å for Ag(4)–O(2)] and angles of O–Ag–O [ranging from 159.86(14)° for O(5)–Ag(2)–O(8) to 161.15(13)° for O(4)–Ag(4)–O(2)] are comparable to values observed in related dimeric structures of reported silver(I) carboxylates.¹¹ The carboxylates from two different L⁻ ligands and two silver(I) centers form a slightly twisted eight-membered ring with an Ag...Ag separation of 2.8031(6) Å for Ag(1)...Ag(2) or 2.8118(6) Å for Ag(3)...Ag(4), which are shorter than the Ag...Ag separation of 2.88 Å in the metallic state, indicating very strong Ag...Ag interactions.^{1a,1b,12} Each L⁻ ligand serves as a μ₃-bridge to link three silver(I) centers through a nitrogen atom and two carboxylate oxygen atoms, respectively, leading to a 2D square-grid-type architecture (Fig. 2a). It should be pointed out that there is no interpenetration between adjacent layers, which facilitated the formation of channels with a diagonal measurement of 10.115(53) and 9.854(39) Å or 10.079(41) and 9.833(48) Å based on the edges of Ag atoms (Fig. 2b). Furthermore, such channels allow the accommodation of a great number of guest water and methanol molecules. The crystal structure of **1** is similar to previous frameworks that do not have interpenetrations between adjacent layers and can provide large void spaces to accommodate solvent molecules or ions,¹³ but it is very different from those with diverse interpenetrations filling the void space.¹⁴

The most salient feature of **1** is that the ligand unsupported Ag...Ag interactions play a crucial role in the construction of the double-layer architecture. Interestingly, the ligand unsupported Ag...Ag interactions [3.0961(7) Å for Ag(2)...Ag(4)#2] are present only in interlayer A (Fig. 3). Besides, together with the Ag...Ag interactions, the presence of π–π interactions, which can be only observed between pyridyl ring A and D [the distance between the centers of rings A–A is 3.727(19) Å; those of rings D–D is 3.710(21) Å], further complete the connections in interlayer A.¹⁵ However, in interlayer B, the Ag...O [2.661(14) Å for Ag(4)...O(4)] interactions also help to support the parallel arrangement of the coordination polymer. This contact is slightly longer than the range of the Ag–O bond distances (2.23–2.52 and 2.17–2.61 for silver(I) carboxylate and oxalate complexes, respectively),^{1a} however, it is still shorter than the sum of van der Waals radii (3.24 Å) of the Ag(I) ion and oxygen atom,¹² implying a significant Ag(I)...O interaction. The shortest Ag...Ag distances [3.774(26) Å for the distance of Ag(4) and Ag(4)] in interlayer B preclude any metal–metal interaction.^{1a} It is worth noting that this alternative stacking mode is the first example of this kind of 2D infinite coordination polymers.

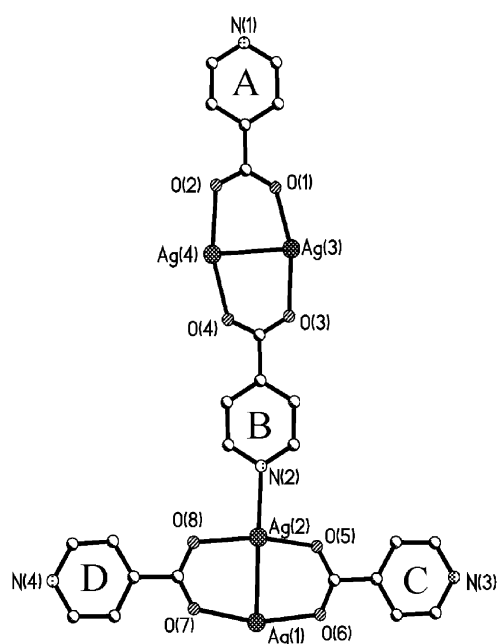
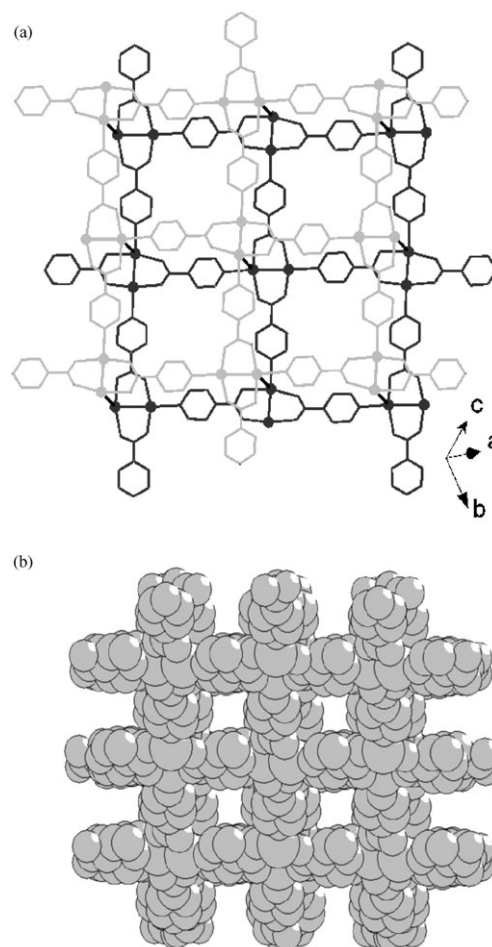
The structure of **2** is shown in Fig. 4 and is similar to [(Ag₃L₂)BF₄]_n (**3**), which has already been reported by Burrows and his co-workers.¹⁶ We obtained **2** from the reaction of isonicotinic acid with AgNO₃, instead of AgBF₄. Recently, according to the research for a rectangular system,¹⁷ the transannular Ag...Ag interaction competes with the interaction between Ag(I) and its anions, and the strength of the Ag...Ag interactions is inversely proportional to their bite sizes. Fortunately, the comparison between **2** and **3** endowed us with an opportunity to explore the effect of counteranions in our system. It can be observed that most Ag...Ag interactions in **3** [ranging from 2.969(5) Å for Ag(1)...Ag(3) to 3.236(5) Å for Ag(2)...Ag(3)] are stronger than those in **2** [ranging from 2.9699(6) for Ag(2)...Ag(3) to 3.2894(6) Å for Ag(1)...Ag(3)], while the Ag...O distance between Ag(I) and NO₃⁻ [ranging from 2.653(9) Å for Ag(2)...O(6) to 3.129(7) Å for

Table 2 Selected bond lengths (Å) and angles (°) for **1** and **2**

1							
Ag(1)–O(7)	2.233(3)	Ag(3)–O(1)	2.253(4)	Ag(2)–O(5)	2.268(3)	Ag(4)–O(4)	2.235(3)
Ag(1)–O(6)	2.253(4)	Ag(3)–O(3)	2.253(4)	Ag(2)–O(8)	2.272(3)	Ag(4)–O(2)	2.283(4)
Ag(1)–N(1)#1	2.319(4)	Ag(3)–N(4)#3	2.325(4)	Ag(2)–N(2)	2.312(4)	Ag(4)–N(3)#4	2.335(4)
Ag(1)–Ag(2)	2.8031(6)	Ag(3)–Ag(4)	2.8118(6)	Ag(2)–Ag(4)#2	3.0961(7)	Ag(4)–Ag(2)#2	3.0961(7)
O(7)–Ag(1)–O(6)	160.75(13)	O(8)–Ag(2)–N(2)	96.16(14)	O(1)–Ag(3)–O(3)	160.81(15)	O(2)–Ag(4)–N(3)#4	93.76(13)
O(7)–Ag(1)–N(1)#1	100.55(14)	O(5)–Ag(2)–Ag(1)	79.50(10)	O(1)–Ag(3)–N(4)#3	98.91(14)	O(4)–Ag(4)–Ag(3)	79.03(9)
O(6)–Ag(1)–N(1)#1	97.82(14)	O(8)–Ag(2)–Ag(1)	85.85(9)	O(3)–Ag(3)–N(4)#3	94.77(14)	O(2)–Ag(4)–Ag(3)	82.34(9)
O(7)–Ag(1)–Ag(2)	79.64(9)	N(2)–Ag(2)–Ag(1)	171.24(10)	O(1)–Ag(3)–Ag(4)	78.08(10)	N(3)#4–Ag(4)–Ag(3)	169.46(10)
O(6)–Ag(1)–Ag(2)	81.39(9)	O(5)–Ag(2)–Ag(4)#2	113.46(11)	O(3)–Ag(3)–Ag(4)	85.01(10)	O(4)–Ag(4)–Ag(2)#2	112.85(9)
N(1)#1–Ag(1)–Ag(2)	172.35(10)	O(8)–Ag(2)–Ag(4)#2	84.94(9)	N(4)#3–Ag(3)–Ag(4)	163.71(10)	O(2)–Ag(4)–Ag(2)#2	62.27(9)
O(5)–Ag(2)–O(8)	159.86(14)	N(2)–Ag(2)–Ag(4)#2	75.69(10)	O(4)–Ag(4)–O(2)	161.15(13)	N(3)#4–Ag(4)–Ag(2)#2	84.48(10)
O(5)–Ag(2)–N(2)	96.38(14)	Ag(1)–Ag(2)–Ag(4)#2	113.014(19)	O(4)–Ag(4)–N(3)#4	104.08(14)	Ag(3)–Ag(4)–Ag(2)#2	85.037(19)
2							
Ag(1)–O(3)#1	2.1356(19)	Ag(1)–Ag(3)	3.2894(6)	Ag(2)–Ag(3)	2.9699(6)	Ag(3)–O(2)	2.1546(18)
Ag(1)–N(2)#2	2.159(2)	Ag(2)–O(4)#1	2.1557(19)	Ag(2)–Ag(2)#3	3.0776(7)	Ag(3)–N(1)	2.183(2)
Ag(1)–Ag(2)	3.0649(6)	Ag(2)–O(1)	2.1648(19)				
O(3)#1–Ag(1)–N(2)#2	175.03(9)	O(4)#1–Ag(2)–O(1)	174.24(8)	O(2)–Ag(3)–Ag(2)	74.86(6)	O(4)#1–Ag(2)–Ag(2)#3	74.09(6)
O(3)#1–Ag(1)–Ag(2)	79.73(6)	O(4)#1–Ag(2)–Ag(3)	89.70(6)	N(1)–Ag(3)–Ag(2)	100.60(6)	O(1)–Ag(2)–Ag(2)#3	108.53(6)
N(2)#2–Ag(1)–Ag(2)	98.19(6)	O(1)–Ag(2)–Ag(3)	85.22(6)	O(2)–Ag(3)–Ag(1)	83.45(6)	Ag(3)–Ag(2)–Ag(2)#3	142.535(14)
O(3)#1–Ag(1)–Ag(3)	87.62(6)	O(4)#1–Ag(2)–Ag(1)	78.44(5)	N(1)–Ag(3)–Ag(1)	96.33(6)	Ag(1)–Ag(2)–Ag(2)#3	77.568(12)
N(2)#2–Ag(1)–Ag(3)	94.94(7)	O(1)–Ag(2)–Ag(1)	96.98(6)	Ag(2)–Ag(3)–Ag(1)	58.369(14)	O(2)–Ag(3)–N(1)	174.83(8)
Ag(2)–Ag(1)–Ag(3)	55.593(10)	Ag(3)–Ag(2)–Ag(1)	66.037(13)				

Symmetry codes: for **1** #1 $x - 2, y - 1, z - 1$; #2 $-x + 1, -y + 2, -z + 2$; #3 $x + 1, y, z + 1$; #4 $x + 1, y + 1, z$; for **2** #1 $-x + 1, -y + 1, -z - 1$; #2 $-x, -y, -z + 1$; #3 $-x + 1, -y, -z$.

Ag(1)···O(6)] in **2** is shorter than the Ag···F distance between Ag(1) and BF₄[−] [ranging from 2.808(6) Å for Ag(1)···F(2) to 3.130(7) Å for Ag(2)···F(4)] in **3**. (Fig. 5) By the same token, the differences of structural data, like those of the transannular system, can also be tentatively attributed to the felicitous combination of size-influence with the electronic effects character. Furthermore, compared to **3**, whose infrared spectrum shows several distinct $\nu(\text{B}-\text{F})$ resonances as opposed to a single broad peak, the reduction of symmetry of the NO₃[−] anion in the solid state was not observed, as evidenced by the bond lengths [1.253(4) Å for O(5)–N(3), 1.256(2) Å for O(6)–N(3) and 1.256(5) Å for O(7)–N(3)] and infrared spectrum, $\nu(\text{N}=\text{O})=$

**Fig. 1** Local coordination environment around Ag atoms in **1**.**Fig. 2** (a) The double-layer grid structure for **1**; (b) space filling views for the channels in **1**. The channels have dimensions with a diagonal measurement of 10.115(53) and 9.854(39) Å or 10.079(41) and 9.833(48) Å based on the edges of Ag atoms. (Guest water and methanol molecules are omitted for clarity.)

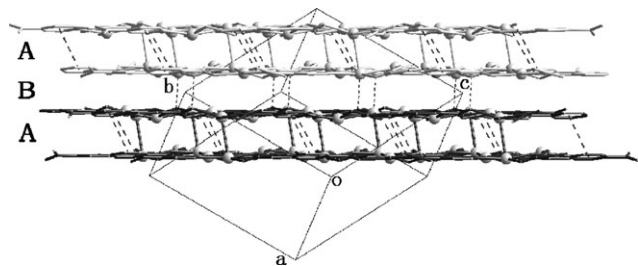


Fig. 3 The ligand unsupported Ag...Ag interactions (thick lines), and π - π interactions (dashed lines) in interlayer A; the Ag...O interactions (dotted lines) in interlayer B.

1384 cm^{-1} . In contrast with F^- in BF_4^- , this phenomenon can be interpreted as the relatively soft nature of O^{2-} in NO_3^- .

Thermal properties

To study the thermal stability of compounds **1** and **2**, thermogravimetric analysis (TGA) was performed on polycrystalline samples under a nitrogen atmosphere. The TGA result of **1** showed a gradual release of all guest water and methanol molecules in the $30\text{--}72^\circ\text{C}$ temperature range (3.63% observed, 3.57% calculated). Subsequent to this, no obvious weight loss was observed up to 274°C . The most significant weight loss occurred from 274 to 302°C , which can be attributed to the complete deposition of the complexes to form Ag_2O as a final product. Considering the formation of stoichiometric amounts of Ag_2O , the conclusion is supported by 50.6% of the residues, which is in accordance with the expected value of 48.6%. The TGA result of **2** showed neither weight loss nor structural change up to about 182°C . Immediately above this point, an obvious weight loss continued in the $182\text{--}302^\circ\text{C}$ temperature range, indicating the collapse of the whole framework. The last residue was also Ag_2O (56.2% observed, 55.2% calculated).

Luminescent properties

Ag(I) complexes usually emit weak photoluminescence at low temperatures, and only a few silver(I) complexes exhibiting luminescent properties at room temperature have been reported.¹⁸ Interestingly, solids **1** and **2** exhibit photoluminescence at room temperature with the emission maximum at *ca.* 548 and 600 nm upon excitation at 358 and 370 nm, respectively (Fig. 6). Noting that HL displayed no luminescence in the solid state at ambient temperature, the intense luminescence in complexes **1** and **2** may be attributed to the silver(I) cluster-based centers therein.^{2,3,19} To our knowledge, because of the impact of the relativistic effect, as well as the coordination structures, the $(n+1)s$ orbitals of d^{10} metal are contracted and therefore have lower energy.^{1b,19d,20,21} A possible assignment for the origin of the emission involves emissive states derived from ligand-to-metal charge transfer (LMCT) transition mixed with d-s character. Presumably, in these complexes, the highest occupied molecular orbital (HOMO) is associated with the silver(I) 4d orbital and the carboxylate group σ orbital, while the lowest unoccupied molecular orbitals (LUMOs) are mainly associated with the silver(I) unoccupied hybrid orbital based on 4d, 5s and 5p, which is similar to the related silver(I) cluster-based coordination complexes reported previously.^{19c-f} It is noteworthy that a band with higher emission energy is observed for **1**, which can be attributed to the larger π -conjugated system in quasi-coplanar layers and the formation of a π - π interaction and Ag...O interactions between adjacent layers, resulting in the energy decrease of HOMO and therefore a larger HOMO-LUMO gap. Hence, the different emission bands may be attributed to different 3D architectures featuring different intensities of supramolecular interactions (such as a π - π interaction and a Ag...O interaction), which may lead to different HOMO-LUMO gaps.²²

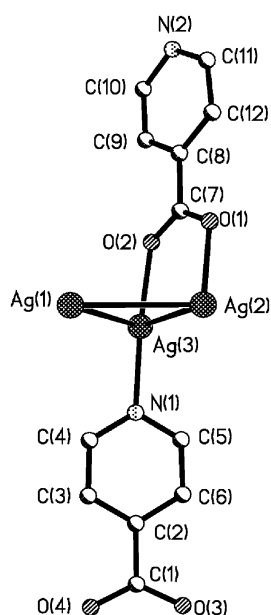


Fig. 4 Local coordination environment around Ag atoms in **2**.

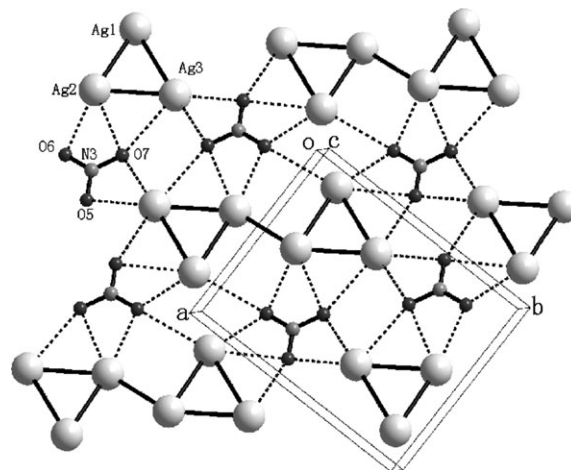


Fig. 5 A section of the structure of polymer **2** showing the interactions between the silver atoms and the NO_3^- anions (dotted lines).

tively (Fig. 6). Noting that HL displayed no luminescence in the solid state at ambient temperature, the intense luminescence in complexes **1** and **2** may be attributed to the silver(I) cluster-based centers therein.^{2,3,19} To our knowledge, because of the impact of the relativistic effect, as well as the coordination structures, the $(n+1)s$ orbitals of d^{10} metal are contracted and therefore have lower energy.^{1b,19d,20,21} A possible assignment for the origin of the emission involves emissive states derived from ligand-to-metal charge transfer (LMCT) transition mixed with d-s character. Presumably, in these complexes, the highest occupied molecular orbital (HOMO) is associated with the silver(I) 4d orbital and the carboxylate group σ orbital, while the lowest unoccupied molecular orbitals (LUMOs) are mainly associated with the silver(I) unoccupied hybrid orbital based on 4d, 5s and 5p, which is similar to the related silver(I) cluster-based coordination complexes reported previously.^{19c-f} It is noteworthy that a band with higher emission energy is observed for **1**, which can be attributed to the larger π -conjugated system in quasi-coplanar layers and the formation of a π - π interaction and Ag...O interactions between adjacent layers, resulting in the energy decrease of HOMO and therefore a larger HOMO-LUMO gap. Hence, the different emission bands may be attributed to different 3D architectures featuring different intensities of supramolecular interactions (such as a π - π interaction and a Ag...O interaction), which may lead to different HOMO-LUMO gaps.²²

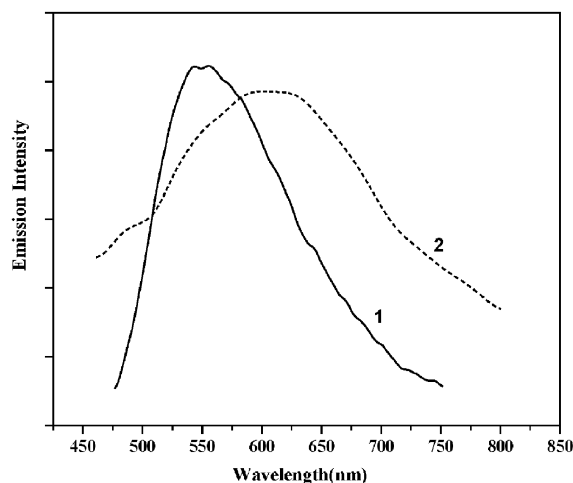


Fig. 6 Fluorescent emission spectra of **1** and **2** in the solid state upon excitation at 358 and 370 nm at room temperature.

Acknowledgements

This work was financially supported by the NSFC (Grant Nos. 20272058 and 20472085) and the program of Science and Technology Plan of Fujian province of China.

References

- (a) M. Jansen, *Angew. Chem., Int. Ed. Engl.*, 1987, **26**, 1098; (b) P. Pyykkö, *Chem. Rev.*, 1997, **97**, 597; (c) M.-L. Tong, X.-M. Chen, B.-H. Ye and L.-N. Ji, *Angew. Chem., Int. Ed.*, 1999, **38**, 2237; (d) O.-S. Jung, S. H. Park, C. H. Park and J. K. Park, *Chem. Lett.*, 1999, 923; (e) Q.-M. Wang and T. C. Mak, *J. Am. Chem. Soc.*, 2001, **123**, 7594; (f) O.-S. Jung, Y. J. Kim, Y.-A. Lee, J. K. Park and H. K. Chae, *J. Am. Chem. Soc.*, 2000, **122**, 9921.
- (a) V. W.-W. Yam, W. K.-M. Fung and K.-K. Cheung, *Chem. Commun.*, 1997, 963; (b) C.-M. Che, Z. Mao, V. M. Miskowski, M.-C. Tse, C.-K. Chan, K.-K. Cheung, D. L. Phillips and K.-H. Leung, *Angew. Chem., Int. Ed.*, 2000, **39**, 4084; (c) C.-M. Che, M.-C. Tse, M. C. W. Chan, K.-K. Cheung, D. L. Phillips and K.-H. Leung, *J. Am. Chem. Soc.*, 2000, **122**, 2464.
- (a) M.-L. Tong and X.-M. Chen, *Inorg. Chem. Commun.*, 2000, **3**, 694; (b) M.-L. Tong, J.-X. Shi and X.-M. Chen, *New J. Chem.*, 2002, **26**, 814; (c) D.-F. Sun, R. Cao, J.-B. Weng, M.-C. Hong and Y.-C. Liang, *J. Chem. Soc., Dalton Trans.*, 2002, 291; (d) J. Fan, W.-Y. Sun, T. Okamura, J. Xie, W.-X. Tang and N. Ueyama, *New J. Chem.*, 2002, **26**, 199.
- K. S. Singh, J. R. Long and P. Stavropoulos, *J. Am. Chem. Soc.*, 1997, **119**, 2942.
- (a) J. Y. Lu and A. M. Babb, *Chem. Commun.*, 2002, 1340; (b) P. Knuuttila, *Polyhedron*, 1984, **3**, 303; (c) R.-G. Xiong, J.-L. Zou, X.-Z. You, H.-K. Fun and S. S. S. Raj, *New J. Chem.*, 1999, **23**, 1051; (d) R.-G. Xiong, S. R. Wilson and W.-B. Lin, *J. Chem. Soc., Dalton Trans.*, 1998, 4098; (e) T.-B. Lu and R. L. Luck, *Acta Crystallogr., Sect. C: Cryst. Struct. Commun.*, 2002, **58**, m152.
- X. Zhang, G.-C. Guo, F.-K. Zheng, G.-W. Zhou, Z.-C. Dong, J.-S. Huang and T. C. W. Mak, *J. Chem. Soc., Dalton Trans.*, 2002, 1344.
- (a) M.-L. Tong, B.-H. Ye, X.-M. Chen and S. W. Ng, *Inorg. Chem.*, 1998, **37**, 2645; (b) M.-L. Tong, S.-L. Zheng and X.-M. Chen, *Chem.-Eur. J.*, 2000, **6**, 3729; (c) S.-L. Zheng, M.-L. Tong and X.-M. Chen, *J. Chem. Soc., Dalton Trans.*, 2001, 586; (d) R.-H. Wang, M.-C. Hong, J.-H. Luo, F.-L. Jiang, L. Han, Z.-Z. Lin and R. Cao, *Inorg. Chim. Acta*, 2004, **357**, 103; (e) S.-L. Zheng, M.-L. Tong and X.-M. Chen, *Coord. Chem. Rev.*, 2003, **246**, 185.
- G. M. Sheldrick, *SHELXTL, Structure Determination Software Package*, Bruker Analytical X-Ray System Inc., Madison, WI, USA, 1997.
- (a) L. Pan, X.-Y. Huang, J. Li, Y.-G. Wu and N.-W. Zheng, *Angew. Chem., Int. Ed.*, 2000, **39**, 527; (b) L. Pan, X.-Y. Huang and J. Li, *J. Solid State Chem.*, 2000, **152**, 236; (c) L. Pan, N. Ching, X.-Y. Huang and J. Li, *Chem.-Eur. J.*, 2001, **7**, 4431.
- (a) B. Cova, A. Briceno and R. Atencio, *New J. Chem.*, 2001, **25**, 1516; (b) F. Jaber, F. Charbonnier, R. Faure and M. Petti-Ramel, *Z. Kristallogr.*, 1994, **209**, 536.
- (a) G. Smith, K. A. Byriel and C. H. L. Kennard, *Aust. J. Chem.*, 1999, **52**, 325; (b) T. C. W. Mak, W.-H. Yip, C. H. L. Kennard, G. Smith and E. J. O'Reilly, *Aust. J. Chem.*, 1986, **39**, 541; (c) G. Smith, A. N. Reddy, K. A. Byriel and C. H. L. Kennard, *J. Chem. Soc., Dalton Trans.*, 1995, 3565; (d) G. Smith and A. N. Reddy, *Polyhedron*, 1994, **13**, 2425; (e) D. Ülkü, M. N. Tahir and E. M. Muvsumov, *Acta Crystallogr., Sect. C: Cryst. Struct. Commun.*, 1996, **52**, 2678.
- A. Bondi, *J. Phys. Chem.*, 1964, **68**, 441.
- (a) M. A. Withersby, A. J. Blake, N. R. Champness, P. Hubberstey, W. S. Li and M. Schröder, *Angew. Chem., Int. Ed. Engl.*, 1997, **36**, 2327; (b) L. R. MacGillivray, R. H. Groeneman and J. L. Atwood, *J. Am. Chem. Soc.*, 1998, **120**, 2676; (c) O. M. Yaghi, H.-L. Li and T. L. Groy, *Inorg. Chem.*, 1997, **36**, 4292.
- (a) H. Gudbjartson, K. Biradha, K. M. Poirier and M. J. Zaworotko, *J. Am. Chem. Soc.*, 1999, **121**, 2599; (b) O. M. Yaghi and H.-L. Li, *J. Am. Chem. Soc.*, 1996, **118**, 295.
- C. Janiak, *J. Chem. Soc., Dalton Trans.*, 2000, 3885.
- A. D. Burrows, M. F. Mahon and M. T. Palmer, *J. Chem. Soc., Dalton Trans.*, 1998, 1941.
- O.-S. Jung, Y. J. Kim, Y.-A. Lee, S. W. Kang and S. N. Choi, *Cryst. Growth Des.*, 2004, **4**, 23.
- (a) S.-L. Zheng, M.-L. Tong, S.-D. Tan, Y. Wang, J.-X. Shi, Y.-X. Tong, H. K. Lee and X.-M. Chen, *Organometallics*, 2001, **20**, 5319; (b) V. W.-W. Yam, K. K.-W. Lo, C.-R. Wang and K.-K. Cheung, *Inorg. Chem.*, 1996, **35**, 5116; (c) V. J. Catalano, H. M. Kar and J. Garnas, *Angew. Chem., Int. Ed.*, 1999, **38**, 1979; (d) D. Fortin, M. Drouin, M. Turcotte and P. D. Harvey, *J. Am. Chem. Soc.*, 1997, **119**, 531.
- (a) G. A. Crosby, R. G. Highland and K. A. Truesdell, *Coord. Chem. Rev.*, 1985, **64**, 41; (b) C. Kutal, *Coord. Chem. Rev.*, 1990, **99**, 213; (c) V. W.-W. Yam, K. K.-W. Lo, W. K.-M. Fung and C.-R. Wang, *Coord. Chem. Rev.*, 1998, **171**, 17; (d) V. W. W. Yam and K. K. W. Lo, *Chem. Soc. Rev.*, 1999, **28**, 323; (e) H. H. Patterson, S. M. Kanan and M. A. Omary, *Coord. Chem. Rev.*, 2000, **208**, 227; (f) V. W.-W. Yam, *Acc. Chem. Res.*, 2002, **35**, 555 and references therein.
- (a) P. Pyykkö, *Chem. Rev.*, 1988, **88**, 563; (b) N. Kaltsoyannis, *J. Chem. Soc., Dalton Trans.*, 1997, 1.
- K. Balasubramanian, *Relativistic Effects in Chemistry Part A: Theory and Techniques; Part B: Applications*, Wiley, New York, 1997.
- (a) P. Cassoux, *Science*, 2001, **291**, 263; (b) A. Kobayashi, H. Tanaka and H. Kobayashi, *J. Mater. Chem.*, 2001, **11**, 2078; (c) S.-L. Zheng, J.-P. Zhang, X.-M. Chen, Z.-L. Huang, Z.-Y. Lin and W.-T. Wong, *Chem.-Eur. J.*, 2003, 3888; (d) S.-L. Zheng, J.-P. Zhang, W.-T. Wang and X.-M. Chen, *J. Am. Chem. Soc.*, 2003, **125**, 6882.